NOTE: Use these buttons to print or save the form. DO NOT use the browser tool bar.

SAVE PRINT

LA-UR-06-4693

Approved for public release;
distribution is unlimited.

Title: Extension of the LAQGSM03 Code to Describe Photo-Nuclear Reactions up to Tens of GeV

Author(s): K. K. Gudima and S. G. Mashnik

Submitted to: Proc. 11th Int. Conf. on Nucl. Reaction Mechanisms, Varenna, Italy, June 12-16, 2006, edited by Ettore Gadioli; E-print: arXiv:nucl-th/0607007; Ricerca Scientifica ed Educazione Permanente, Supplemento N. 126, 2006, pp. 525-534

SAVE PRINT CLEAR FORM

Los Alamos
NATIONAL LABORATORY

Los Alamos National Laboratory, an affirmative action/equal opportunity employer, is operated by the University of California for the U.S. Department of Energy under contract W-7405-ENG-36. By acceptance of this article, the publisher recognizes that the U.S. Government retains a nonexclusive, royalty-free license to publish or reproduce the published form of this contribution, or to allow others to do so, for U.S. Government purposes. Los Alamos National Laboratory requests that the publisher identify this article as work performed under the auspices of the U.S. Department of Energy. Los Alamos National Laboratory strongly supports academic freedom and a researcher's right to publish; as an institution, however, the Laboratory does not endorse the viewpoint of a publication or guarantee its technical correctness.

Form 836 (8/00)

Extension of the LAQGSM03.01 Code to Describe Photo-Nuclear Reactions up to Tens of GeV

K. K. Gudima[1] and S. G. Mashnik[2]

[1]*Institute of Applied Physics, Academy of Science of Moldova, Chişinău, Moldova*
[2]*X-3-MCC, Los Alamos National Laboratory, Los Alamos, NM 87545, USA*

Abstract

The Los Alamos version of the Quark-Gluon String Model implemented in the code LAQGSM03 was extended to describe photonuclear reactions at energies up to tens of GeV. We have incorporated 56 channels to consider γp elementary interactions during the cascade stage of reactions and 56 channels for γn interactions, in addition to absorption of photons on two-nucleon pairs, into LAQGSM03 and have tested the extended code referred to as LAQGSM03.01 on a number of measured high-energy photonuclear reactions. Here, we present the photonuclear reaction model of LAQGSM03.01 and show examples of its results compared with available experimental data.

1. Introduction

Following an increased interest in nuclear data for such projects as the Accelerator Transmutation of nuclear Wastes (ATW), Accelerator Production of Tritium (APT), Spallation Neutron Source (SNS), Rare Isotope Accelerator (RIA), Proton Radiography (PRAD) as a radiographic probe for the Advanced Hydro-test Facility and others, for several years the US Department of Energy has supported our work on the development of improved versions of the Cascade-Exciton Model (CEM) of nuclear reactions [1, 2] and the Los Alamos version of the Quark-Gluon String Model (LAQGSM) [3, 4] to describe reactions induced by particles and nuclei at energies up to about 1 TeV/nucleon [5]-[9]. To describe fission and production of light fragments heavier than ^{4}He, we have merged both our codes with several evaporation/fission/fragmentation models, including the Generalized Evaporation/fission Model code GEM2 by Furihata [10], the fission-like binary-decay code GEMINI by Charity *et al.* [11], and the Statistical Multifragmentation Model (SMM) by Botvina *et al.* [12]. Our codes perform as well as and often better than other current models in describing a large variety of spallation, fission, and fragmentation reactions, therefore they are used as event-generators in several transport codes.

However, the initial version of the Los Alamos Quark-Gluon String Model (LAQGSM) [3], just like its precursor, the Quark-Gluon String Model (QGSM) [13], did not consider photonuclear reactions, while its 2003 version, LAQGSM03 [1], describes such reactions only for energies up to about 1.5 GeV. This is not convenient when using our codes to solve problems for PRAD, NASA, and other high-energy applications or to analyze future high-energy measurements at the Thomas Jefferson National Accelerator Facility (CEBAF), where photons with much higher energy are created and need to be simulated with our even-generators in transport codes like MCNP6 [14], MARS [15], MCNPX [16], and others. To address this problem, we have extended [8] LAQGSM03.01 to describe photonuclear reactions up to tens of GeV. The next section presents a short description of the high-energy photonuclear reaction model of LAQGSM03.01, followed by two sections with examples of calculated particle spectra, yields, and recoil properties of products from high-energy photonuclear reactions compared with available data.

2. High-Energy Photonuclear Model of LAQGSM03.01

Initially [1], an improved version of the Dubna InraNuclear cascade photonuclear reaction model developed originally 37 years ago by one of us in collaboration with Iljinov and Toneev [17] to describe photonuclear reactions at energies above the Giant Dipole Resonance (GDR) region was incorporated into LAQGSM. [At photon energies $T_\gamma = 10$–40 MeV, the de Broglie wavelength $\lambdabar$ is of the order of 20–5 fm, greater than the average inter-nucleonic distance in the nucleus; the photons interact with the nuclear dipole resonance as a whole, thus the INC is not applicable.] Below the pion production threshold, the Dubna INC considers absorption of photons on "quasi-deuteron" pairs according to the Levinger model [18]:

$$\sigma_{\gamma A} = L\frac{Z(A-Z)}{A}\sigma_{\gamma d} \ , \tag{1}$$

where A and Z are the mass and charge numbers of the nucleus, $L \approx 10$, and $\sigma_{\gamma d}$ is the total photoabsorption cross section on deuterons as defined from experimental data.

At photon energies above the pion-production threshold, the Dubna INC considers production of only one or two pions (channels #1–3 and 15–17 from Table 1); the concrete mode of the reaction is chosen by the Monte Carlo method according to the partial cross sections, defined from available experimental data. This limits the use of such an approach to photon energies of only up to about 1.5 GeV, as contribution from multiple pion production become predominant at higher energies.

To address this problem, we have extended LAQGSM03 [1] to describe photonuclear reactions at energies up to tens of GeV. For this, we took advantage of the high-energy event generators for γp and γn elementary interactions from the Moscow high-energy photonuclear reaction model [19] kindly sent us by one of its coauthors, Dr. Igor Pshenichnov. Let us note that the γp and γn event generators from the Moscow INC [19] use an improvement and extension to higher energies of the Genova γp and γn event generators developed by P. Corvisiero *et al.* to describe photon-nucleon interactions up to 4 GeV [20]. We have incorporated into LAQGSM03.01 56 channels to consider γp elementary interactions during the cascade stage of reactions, and 56 channels for γn interactions. These reaction channels new to LAQGSM03.01 are listed in Table 1 (its precursor, LAQGSM03 [1], considers only channels #1–3 and 15–17, and only up to about 1.5 GeV).

To describe in LAQGSM03.01 the two-body channels #1–14, we use part of a file containing smooth approximations through presently available experimental data sent us by Dr. Pshenichnov but have developed our own algorithms and written our own routines to simulate unambiguously $d\sigma/d\Omega$ and to choose the corresponding value of Θ for any E_γ, using a single random number ξ uniformly distributed in the interval [0,1], as described in [1]. Fig. 1 shows examples of angular distributions of π^0 from $\gamma p \to \pi^0 p$ interactions as functions of $\Theta^{\pi}_{c.m.s}$ at eight different photon energies as simulated by our routines compared with available experimental data. Examples of similar distributions for π^+ from $\gamma p \to \pi^+ n$ interactions may be found in [1].

To describe the channels #15–21 with two and three pions in the final state, we use the γp and γn event generators send us by Dr. Pshenichnov, but use our own interpolation for integral cross sections. We do not show here examples of cross sections for these channels, as we reproduce with LAQGSM03.01 all the results by Pshenichnov *et al.* shown in Figs. 6 and 8 of Ref. [19].

Finally, to describe in LAQGSM03.01 the multi-pion channels #22–56, we use the isospin statistical model as realized in the γp and γn event generators send us by Dr. Pshenichnov and described in details in [19], without any changes. For channels #22–56, we reproduce exactly in LAQGSM03.01 the results by Pshenichnov *et al.* as published in Ref. [19], therefore we do not show here examples of such results.

After the bombarding photon is absorbed by two nucleons or interacts inelastically with a nucleon according the channels #1–56, we get inside the nucleus several "secondary" cascade nucleons, pions, or other mesons and resonances listed in Table 1, depending on which channel is simulated from the corresponding cross sections at the given photon energy to actually occur. These "secondary" cascade particles interact further with inranuclear nucleons or leave the nucleus, depending on their coordinates and momenta. The further behavior of the reaction starting from this stage, after the photon had "disappeared", is described by LAQGSM03.01 exactly the same way as for any other types of reactions, induced, e.g., by nucleons or heavy ions.

LAQGSM03.01 [8] is the latest modification of the Los Alamos version of the Quark-Gluon String Model [3], which in its turn is an improvement of the Quark-Gluon String Model [13]. It describes reactions induced by both particles and nuclei as a three-stage process: IntraNuclear Cascade (INC), followed by preequilibrium emission of particles during the equilibration of the excited residual nuclei formed after the INC, followed by evaporation of particles from or fission of the compound nuclei. The INC stage of reactions is described with a recently improved version [8] of the time-depending intranuclear cascade model developed initially at Dubna, often referred in the literature simply as the **D**ubna intranuclear **C**ascade **M**odel, DCM (see [21] and references therein). The preequilibrium part of reactions is described with the last version of the Modified Exciton Model (MEM) from the improved Cascade-Exciton Model (CEM) code CEM03.01 [2]. The evaporation and fission stages of reactions are calculated with an updated and improved version of the Generalized Evaporation Model code GEM2 by Furihata [10], which considers evaporation of up to 66 types of different particles and light fragments (up to ^{28}Mg). If the excited residual nucleus produced after the INC has a mass number $A < 13$, LAQGSM03.01 uses a recently updated and improved version of the Fermi Break-up model (in comparison with the initial version developed in the group of Prof. V. S. Barashenkov at JINR, Dubna and used in QGSM [13]

Table 1. Channels of elementary γN interactions taken into account in LAQGSM03.01

#	γp-interactions	γn-interactions
1	$\gamma p \to \pi^+ n$	$\gamma n \to \pi^- p$
2	$\gamma p \to \pi^0 p$	$\gamma n \to \pi^0 n$
3	$\gamma p \to \Delta^{++} \pi^-$	$\gamma n \to \Delta^+ \pi^-$
4	$\gamma p \to \Delta^+ \pi^0$	$\gamma n \to \Delta^0 \pi^0$
5	$\gamma p \to \Delta^0 \pi^+$	$\gamma n \to \Delta^- \pi^+$
6	$\gamma p \to \rho^0 p$	$\gamma n \to \rho^0 n$
7	$\gamma p \to \rho^+ n$	$\gamma n \to \rho^- p$
8	$\gamma p \to \eta p$	$\gamma n \to \eta n$
9	$\gamma p \to \omega p$	$\gamma n \to \omega n$
10	$\gamma p \to \Lambda K^+$	$\gamma n \to \Lambda K^0$
11	$\gamma p \to \Sigma^0 K^+$	$\gamma n \to \Sigma^0 K^0$
12	$\gamma p \to \Sigma^+ K^0$	$\gamma n \to \Sigma^- K^+$
13	$\gamma p \to \eta' p$	$\gamma n \to \eta' n$
14	$\gamma p \to \phi p$	$\gamma n \to \phi n$
15	$\gamma p \to \pi^+ \pi^- p$	$\gamma n \to \pi^+ \pi^- n$
16	$\gamma p \to \pi^0 \pi^+ n$	$\gamma n \to \pi^0 \pi^- p$
17	$\gamma p \to \pi^0 \pi^0 p$	$\gamma n \to \pi^0 \pi^0 n$
18	$\gamma p \to \pi^0 \pi^0 \pi^0 p$	$\gamma n \to \pi^0 \pi^0 \pi^0 n$
19	$\gamma p \to \pi^+ \pi^- \pi^0 p$	$\gamma n \to \pi^+ \pi^- \pi^0 n$
20	$\gamma p \to \pi^+ \pi^0 \pi^0 n$	$\gamma n \to \pi^- \pi^0 \pi^0 p$
21	$\gamma p \to \pi^+ \pi^+ \pi^- n$	$\gamma n \to \pi^+ \pi^- \pi^- p$
22	$\gamma p \to \pi^0 \pi^0 \pi^0 \pi^0 p$	$\gamma n \to \pi^0 \pi^0 \pi^0 \pi^0 n$
23	$\gamma p \to \pi^+ \pi^- \pi^0 \pi^0 p$	$\gamma n \to \pi^+ \pi^- \pi^0 \pi^0 n$
24	$\gamma p \to \pi^+ \pi^+ \pi^- \pi^- p$	$\gamma n \to \pi^+ \pi^+ \pi^- \pi^- n$
25	$\gamma p \to \pi^+ \pi^0 \pi^0 \pi^0 n$	$\gamma n \to \pi^- \pi^0 \pi^0 \pi^0 p$
26	$\gamma p \to \pi^+ \pi^+ \pi^- \pi^0 n$	$\gamma n \to \pi^+ \pi^- \pi^- \pi^0 p$
27	$\gamma p \to \pi^0 \pi^0 \pi^0 \pi^0 \pi^0 p$	$\gamma n \to \pi^0 \pi^0 \pi^0 \pi^0 \pi^0 n$
28	$\gamma p \to \pi^+ \pi^- \pi^0 \pi^0 \pi^0 p$	$\gamma n \to \pi^+ \pi^- \pi^0 \pi^0 \pi^0 n$
29	$\gamma p \to \pi^+ \pi^+ \pi^- \pi^- \pi^0 p$	$\gamma n \to \pi^+ \pi^+ \pi^- \pi^- \pi^0 n$
30	$\gamma p \to \pi^+ \pi^0 \pi^0 \pi^0 \pi^0 n$	$\gamma n \to \pi^- \pi^0 \pi^0 \pi^0 \pi^0 p$
31	$\gamma p \to \pi^+ \pi^+ \pi^- \pi^0 \pi^0 n$	$\gamma n \to \pi^+ \pi^- \pi^- \pi^0 \pi^0 p$
32	$\gamma p \to \pi^+ \pi^+ \pi^+ \pi^- \pi^- n$	$\gamma n \to \pi^+ \pi^+ \pi^- \pi^- \pi^- p$
33	$\gamma p \to \pi^0 \pi^0 \pi^0 \pi^0 \pi^0 \pi^0 p$	$\gamma n \to \pi^0 \pi^0 \pi^0 \pi^0 \pi^0 \pi^0 n$
34	$\gamma p \to \pi^+ \pi^- \pi^0 \pi^0 \pi^0 \pi^0 p$	$\gamma n \to \pi^+ \pi^- \pi^0 \pi^0 \pi^0 \pi^0 n$
35	$\gamma p \to \pi^+ \pi^+ \pi^- \pi^- \pi^0 \pi^0 p$	$\gamma n \to \pi^+ \pi^+ \pi^- \pi^- \pi^0 \pi^0 n$
36	$\gamma p \to \pi^+ \pi^+ \pi^+ \pi^- \pi^- \pi^- p$	$\gamma n \to \pi^+ \pi^+ \pi^+ \pi^- \pi^- \pi^- n$
37	$\gamma p \to \pi^+ \pi^0 \pi^0 \pi^0 \pi^0 \pi^0 n$	$\gamma n \to \pi^- \pi^0 \pi^0 \pi^0 \pi^0 \pi^0 p$
38	$\gamma p \to \pi^+ \pi^+ \pi^- \pi^0 \pi^0 \pi^0 n$	$\gamma n \to \pi^+ \pi^- \pi^- \pi^0 \pi^0 \pi^0 p$
39	$\gamma p \to \pi^+ \pi^+ \pi^+ \pi^- \pi^- \pi^0 n$	$\gamma n \to \pi^+ \pi^+ \pi^- \pi^- \pi^- \pi^0 p$
40	$\gamma p \to \pi^0 \pi^0 \pi^0 \pi^0 \pi^0 \pi^0 \pi^0 p$	$\gamma n \to \pi^0 \pi^0 \pi^0 \pi^0 \pi^0 \pi^0 \pi^0 n$
41	$\gamma p \to \pi^+ \pi^- \pi^0 \pi^0 \pi^0 \pi^0 \pi^0 p$	$\gamma n \to \pi^+ \pi^- \pi^0 \pi^0 \pi^0 \pi^0 \pi^0 n$
42	$\gamma p \to \pi^+ \pi^+ \pi^- \pi^- \pi^0 \pi^0 \pi^0 p$	$\gamma n \to \pi^+ \pi^+ \pi^- \pi^- \pi^0 \pi^0 \pi^0 n$
43	$\gamma p \to \pi^+ \pi^+ \pi^+ \pi^- \pi^- \pi^- \pi^0 p$	$\gamma n \to \pi^+ \pi^+ \pi^+ \pi^- \pi^- \pi^- \pi^0 n$
44	$\gamma p \to \pi^+ \pi^0 \pi^0 \pi^0 \pi^0 \pi^0 \pi^0 n$	$\gamma n \to \pi^- \pi^0 \pi^0 \pi^0 \pi^0 \pi^0 \pi^0 p$
45	$\gamma p \to \pi^+ \pi^+ \pi^- \pi^0 \pi^0 \pi^0 \pi^0 n$	$\gamma n \to \pi^+ \pi^- \pi^- \pi^0 \pi^0 \pi^0 \pi^0 p$
46	$\gamma p \to \pi^+ \pi^+ \pi^+ \pi^- \pi^- \pi^0 \pi^0 n$	$\gamma n \to \pi^+ \pi^+ \pi^- \pi^- \pi^- \pi^0 \pi^0 p$
47	$\gamma p \to \pi^+ \pi^+ \pi^+ \pi^+ \pi^+ \pi^- \pi^- \pi^- n$	$\gamma n \to \pi^+ \pi^+ \pi^+ \pi^- \pi^- \pi^- \pi^- \pi^- p$
48	$\gamma p \to \pi^0 \pi^0 \pi^0 \pi^0 \pi^0 \pi^0 \pi^0 \pi^0 p$	$\gamma n \to \pi^0 \pi^0 \pi^0 \pi^0 \pi^0 \pi^0 \pi^0 \pi^0 n$
49	$\gamma p \to \pi^+ \pi^- \pi^0 \pi^0 \pi^0 \pi^0 \pi^0 \pi^0 p$	$\gamma n \to \pi^+ \pi^- \pi^0 \pi^0 \pi^0 \pi^0 \pi^0 \pi^0 n$
50	$\gamma p \to \pi^+ \pi^+ \pi^- \pi^- \pi^0 \pi^0 \pi^0 \pi^0 p$	$\gamma n \to \pi^+ \pi^+ \pi^- \pi^- \pi^0 \pi^0 \pi^0 \pi^0 n$
51	$\gamma p \to \pi^+ \pi^+ \pi^+ \pi^- \pi^- \pi^- \pi^0 \pi^0 p$	$\gamma n \to \pi^+ \pi^+ \pi^+ \pi^- \pi^- \pi^- \pi^0 \pi^0 n$
52	$\gamma p \to \pi^+ \pi^+ \pi^+ \pi^+ \pi^+ \pi^- \pi^- \pi^- \pi^- p$	$\gamma n \to \pi^+ \pi^+ \pi^+ \pi^+ \pi^+ \pi^- \pi^- \pi^- \pi^- n$
53	$\gamma p \to \pi^+ \pi^0 \pi^0 \pi^0 \pi^0 \pi^0 \pi^0 \pi^0 n$	$\gamma n \to \pi^- \pi^0 \pi^0 \pi^0 \pi^0 \pi^0 \pi^0 \pi^0 p$
54	$\gamma p \to \pi^+ \pi^+ \pi^- \pi^0 \pi^0 \pi^0 \pi^0 \pi^0 n$	$\gamma n \to \pi^+ \pi^- \pi^- \pi^0 \pi^0 \pi^0 \pi^0 \pi^0 p$
55	$\gamma p \to \pi^+ \pi^+ \pi^+ \pi^- \pi^- \pi^0 \pi^0 \pi^0 n$	$\gamma n \to \pi^+ \pi^+ \pi^- \pi^- \pi^- \pi^0 \pi^0 \pi^0 p$
56	$\gamma p \to \pi^+ \pi^+ \pi^+ \pi^+ \pi^- \pi^- \pi^- \pi^- \pi^0 n$	$\gamma n \to \pi^+ \pi^+ \pi^+ \pi^- \pi^- \pi^- \pi^- \pi^- \pi^0 p$

and described in [22]) to calculate its decay instead of considering a preequilibrium stage followed by evaporation from compound nuclei, as described above. LAQGSM03.01 considers also coalescence of complex particles up to ^{4}He from energetic nucleons emitted during the INC, using an updated coalescence model in comparison with the version described in [21].

We have developed also "S" and "G" versions of LAQGSM03.01, namely: LAQGSM03.S1 and LAQGSM03.G1 [9]. LAQGSM03.S1 [9] is exactly the same as LAQGSM03.01, but considers also multifragmentation of excited nuclei produced after the preequilibrium stage of reactions, when their excitation energy is above 2A MeV, using the Statistical Multifragmentation Model (SMM) by Botvina *et al.* [12] (the 'S" in the extension of LAQGSM03.S1 stands for SMM). LAQGSM03.G1 [9] is exactly the same as LAQGSM03.01, but uses the fission-like binary-decay model GEMINI of Charity *et al.* [11], which considers evaporation of all possible fragments, instead of using the GEM2 model [10] (the "G" stands for GEMINI).

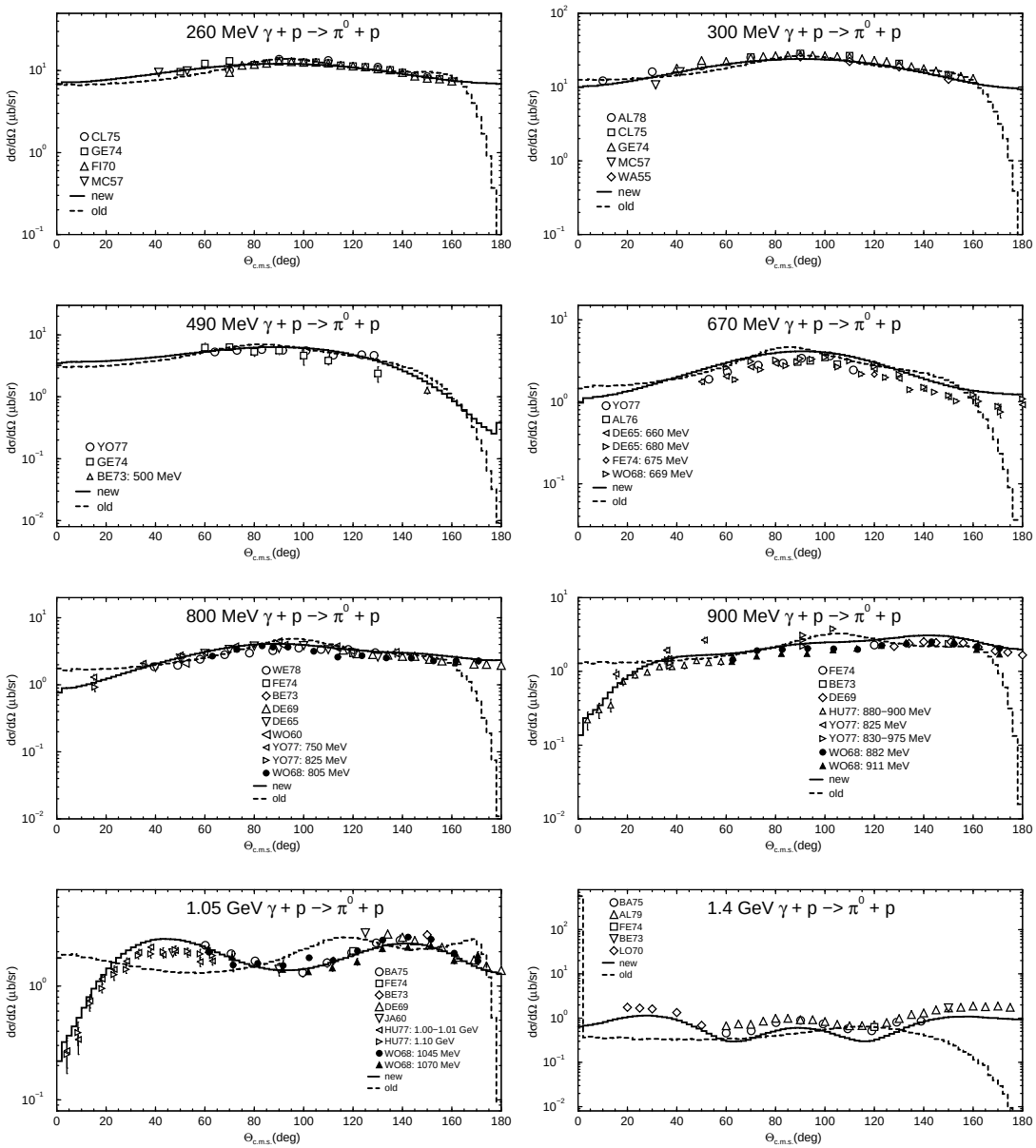

Figure 1. Example of eight angular distributions of π^0 from $\gamma p \to \pi^0 p$ as functions of $\Theta^{\pi}_{c.m.s}$ at photon energies from 260 MeV to 1.4 GeV. The dashed lines show the old approximations of the Dubna INC [17] while the solid lines are our new approximations incorporated into LAQGSM03.01 (and into CEM03 and LAQGSM03 [1]). References to experimental data shown by different symbols may be found in our recent work [1].

3. Particle Spectra

We have tested LAQGSM03.01 and its "S" and "G" versions extended to describe high-energy photonuclear reactions against practically all experimental data above 1 GeV we were able to find in the literature, but we limit ourselves here to presenting only several exemplary results.

Let us start with comparing results by LAQGSM03.01 with experimental data at relatively low energies, of about 1 GeV, where other photonuclear models also do work, then move gradually to reactions at higher energies. Figure 2 presents examples of proton spectra from bremsstrahlung interaction with carbon at $E^{max} = 1050$ MeV. One can see that LAQGSM03.01 describes as well as CEM03.01 does the measured proton spectra and agrees with the data better than the direct knockout model [24] and the quasi-deuteron calculations [25] do.

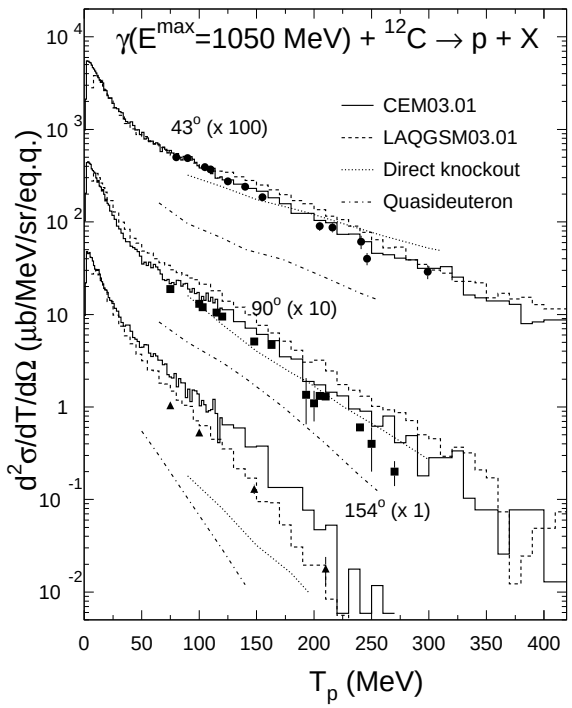

Figure 2. Comparison of measured [23] differential cross section for proton photoproduction on carbon at 43°, 90°, and 154° by bremsstrahlung photons with $E^{max} = 1.05$ GeV (symbols) with CEM03.01 (solid histograms) and LAQGSM03.01 (dashed histograms), and predictions by the direct knockout model [24] (dotted lines) and a quasi-deuteron calculation [25] (dot-dashed lines), respectively. The experimental data and results by the direct knockout and quasi-deuteron models are taken from Fig. 5 of Ref. [24].

Figure 3 presents examples of proton and pion spectra from photonuclear reactions at higher energies, namely proton spectra at 60, 90, and 150 degrees from interaction of bremsstrahlung γ quanta of maximum energy $E^{max} =$ 2.0, 3.0, and 4.5 GeV with ^{12}C, ^{27}Al, ^{63}Cu, and ^{208}Pb and pion spectra from interaction of the same bremsstrahlung γ quanta with ^{12}C, ^{63}Cu, and ^{208}Pb. These reactions are of a higher interest to us than the one presented in Fig. 2 for the following reason: The proton and pion spectra presented in Fig. 3 were measured more than 25 years ago at the Yerevan Physics Institute [26]-[29] with a major hope of revealing some "exotic" or unknown mechanisms of nuclear reactions leading to the production of so called "cumulative" (*i.e.*, kinematically forbidden for quasi-free intranuclear projectile-nucleon collisions) particles. At the time the measurements [26]-[29] were done, there were not high-energy photonuclear reaction models available in the literature, therefore these data were not analyzed so far by any models. We do not know of any publication or oral presentation where these measurements were reproduced by a theoretical model, event generator, or transport code. It is noteworthy that LAQGSM03.01 describes quite well all the spectra measured both in the cumulative and non-cumulative regions (as it does, e.g., for particles emitted from interaction of 400 GeV protons with nuclei; see [7] for details) in a single approach, without any fitting or free parameters, and without involving any "exotic" reaction mechanisms.

These results do not imply, of course, that the γ- or proton-nucleus interaction physics is completely described by the reaction mechanisms considered by LAQGSM03.01. Our present results do not exclude some contribution to the production of these particles from other reaction mechanisms not considered by LAQGSM03.01. But the contribution from "exotic" mechanisms to cumulative particle production from these high-energy reactions seems to be small; inclusive particle spectra are not sensitive enough for an unambiguous determination of the mechanisms of particle production, just as observed heretofore at intermediate and low energies [30].

4. Product Yields and Recoil Properties

This section presents several examples of cross sections (yields) of the nuclides produced in high-energy photonuclear reactions and of their recoil properties. Fig. 4 shows a comparison of the measured

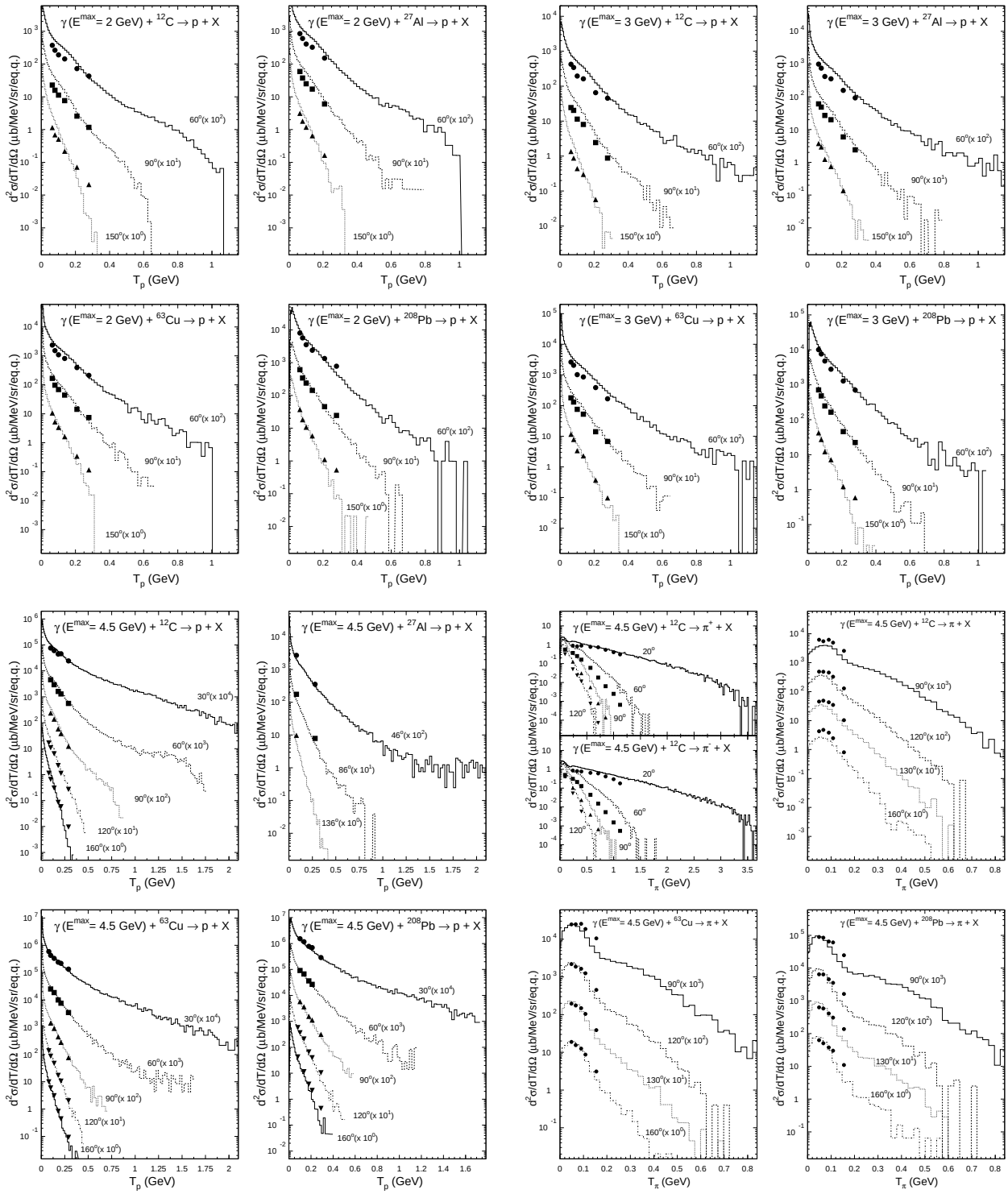

Figure 3. Proton spectra at 60, 90, and 150 degrees from interaction of bremsstrahlung γ quanta of maximum energy $E^{max} = 2.0$, 3.0, and 4.5 GeV with ^{12}C, ^{27}Al, ^{63}Cu, and ^{208}Pb (left and right top panels and left bottom panel of four plots). Spectra of π^+ and π^- produced by $E^{max} = 4.5$ GeV bremsstrahlung on ^{12}C and spectra of charged pions (both π^+ and π^-) from interaction of the same bremsstrahlung γ quanta with ^{12}C, ^{63}Cu, and ^{208}Pb (right bottom panel of four plots). Experimental values shown by symbols are from [26]-[29] while histograms show results by LAQGSM03.01. To the best of our knowledge, we are able to describe these data with LAQGSM03.01 for the first time (see text).

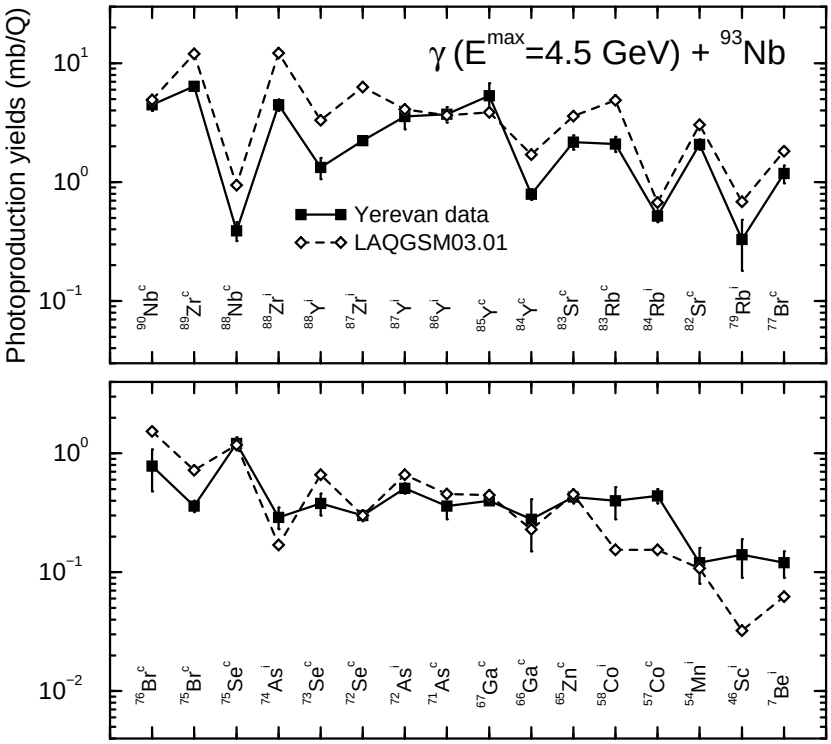

Figure 4. Detailed comparison between experimental yields [31] and those calculated by LAQGSM03.01 of radioactive products from the interaction of bremsstrahlung γ quanta of maximum energy 4.5 GeV with ^{93}Nb. The cumulative yields are labeled as "c" while the independent cross sections, as "i". To the best of our knowledge, using LAQGSM03.01 we are able to describe these data for the first time.

production cross sections from interaction of bremsstrahlung γ quanta of maximum energy 4.5 GeV with ^{93}Nb [31] with results by LAQGS03.01. We see that LAQGSM03.01 describes most of the measured yields quite well, with only several cases when the calculations differ from the data within a factor of two to three, that is also not too bad, considering that all calculations are in the absolute value, without any fitting of parameters or normalization.

Fig. 5 shows a similar reaction, induced by $E^{max} = 4.5$ GeV bremsstrahlung on ^{65}Cu, but measured regarding the recoil properties of the produced nuclides [32]. No product yields were measured from this reaction, so the top-left plot in Fig. 5 shows only predictions by LAQGSM03.01 and its "S" and "G" versions for this quantity. The left plot in the middle row of Fig. 5 shows predictions by LAQGSM03.01 and its "S" and "G" versions for the mean laboratory angle of products. We see quite a big difference for this characteristics between predictions by versions of the model with different treatment of the evaporation stage of reaction (compare the "standard", LAQGSM03.01, results that uses GEM2 with results by its "G" version that uses GEMINI) and between results calculated without (LAQGSM0.01) and with taking into account multifragmentation of highly-excited compound nuclei (LAQGSM03.S1). Unfortunately, this quantity was not measured and we can not uncover the "real" reaction mechanisms based on these results until experimental data are available.

The other three plots in Fig. 5 show results by LAQGSM03.01 and its "G" and "S" versions for the Z-averaged A-dependence of the mean laboratory velocity v_z of products, the R=F/B ratio of the forward product cross sections to the backward ones, and their mean laboratory kinetic energy compared with available data [32]. We see a very good agreement between calculations and the data for the mean kinetic energy, a not so good agreement for the mean parallel velocity v_z of products, and a poor agreement for R=F/B. Let us note that in the experimental work [32], these characteristics were measured only for several final isotopes, while results of calculations shown in Fig. 5 are for the Z-averaged A-dependence of all possible products. If to compare the data with calculations for only the measured products, isotope-by-isotope, the agreement between measurements and calculations becomes better. However, as can be seen from Fig. 6, there is still some disagreement between experimental data and theoretical results by all three versions of LAQGSM considered here for the values of R=F/B, similar to results obtained for reactions induced by protons and deuterons [33]. In making such comparisons, we first recognize that the experiment and the calculations differ in that: 1) the experimental data were extracted assuming the "two-step vector model" (see references and details in [32, 33]), while the LAQGSM calculations were done without the assumptions of this model; 2) the measurements were performed on foils (thick targets), while the calculations were done for interactions of photons (protons and deuterons, in the case of Ref. [33]) with nuclei (thin targets). These differences must be considered before assessing possible deficiencies in the models.

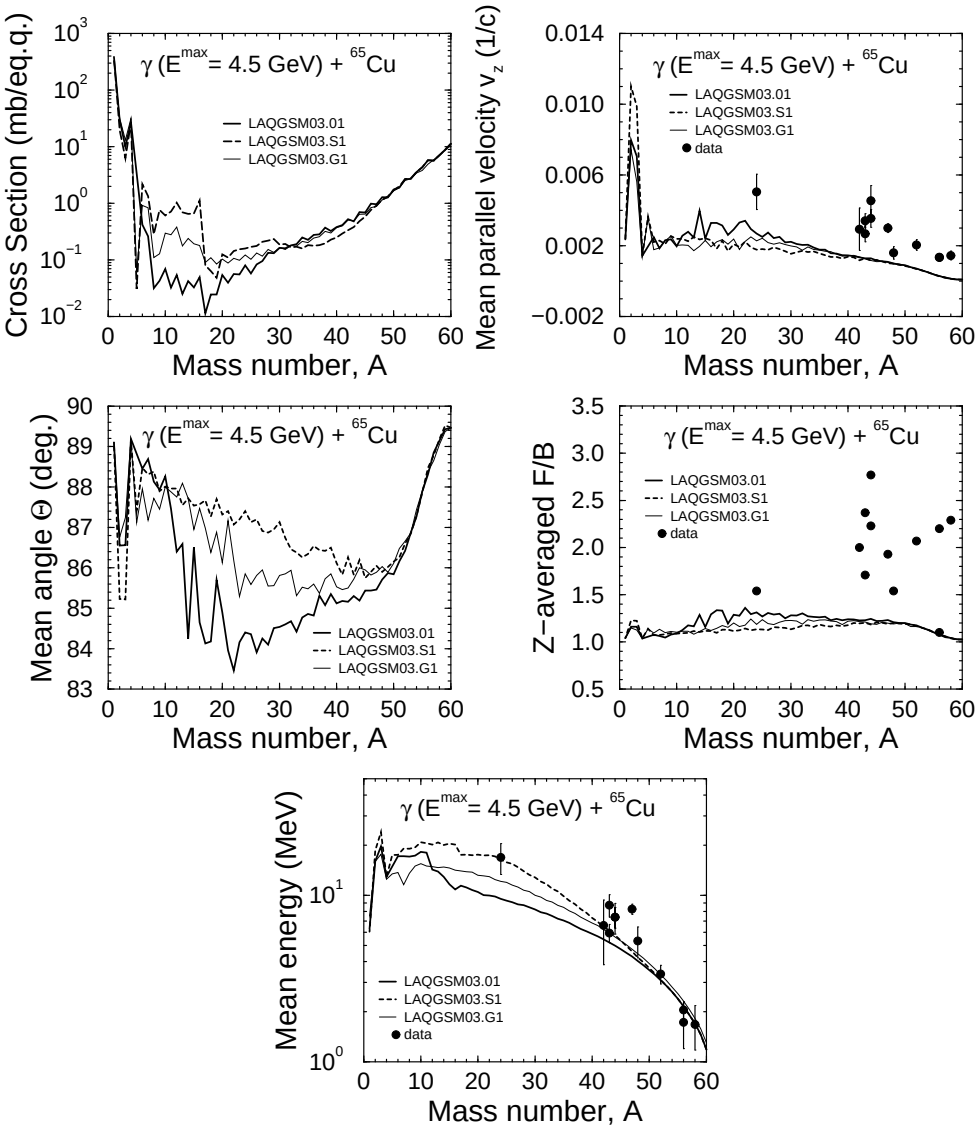

Figure 5. Results by LAQGSM03.01 and its "S" and "G" versions for the Z-averaged A-dependence of the mass yield of all products, their mean parallel laboratory velocity v_z in the beam direction, their mean laboratory angle Θ, the R=F/B ratio of the forward product cross sections to the backward ones, and their mean laboratory kinetic energy for the reaction of $E^{max} = 4.5$ GeV bremsstrahlung photons on ^{65}Cu compared with available experimental data by Arakelyan *et al.* [32].

Finally, Fig. 7 shows a comparison of the calculated by LAQGSM03.01 mass distribution of products with experimental data for the highest energy we were able to find data in the literature, namely for the reaction $E^{max} = 6$ GeV bremsstrahlung gammas on ^{238}U [34, 35]. We see a good agreement between the calculations and these high-energy photonuclear reaction data.

To conclude, let us note that to the best of our knowledge, we were able to describe with LAQGSM03.01 all the reactions discussed in this section for the first time: We do not know of any publication or oral presentation where these experimental data were reproduced by a theoretical model, event generator, or transport code.

5. Summary

The latest modification of the Los Alamos Quark-Gluon String Model released in the code LAQGSM03.01 and its "S" and "G" versions were extended to describe photonuclear reactions at energies up to tens of GeV. We have tested our high-energy photonuclear models against practically all experimental data above 1 GeV we were able to find in the literature and can conclude that they describe the measured data reasonably well, without re-fitting any parameters. Our models are not yet ready to describe properly reactions induced by gammas of tens of MeV, in the GDR region (though they provide not completely wrong results even at such low energies; see, e.g., [1]). We are developing now approximations for the GDR region, to extend the use of our codes for low-energy photonuclear reactions as well. LAQGSM03.01 was incorporated recently into the transport code MARS [15] and is currently being incorporated into MCNP6 [14] and MCNPX [16]. This would allow others to use LAQGSM03.01 as an event-generator in these transport codes to simulate high-energy photonuclear reactions with targets of practically arbitrary geometry and nuclide composition.

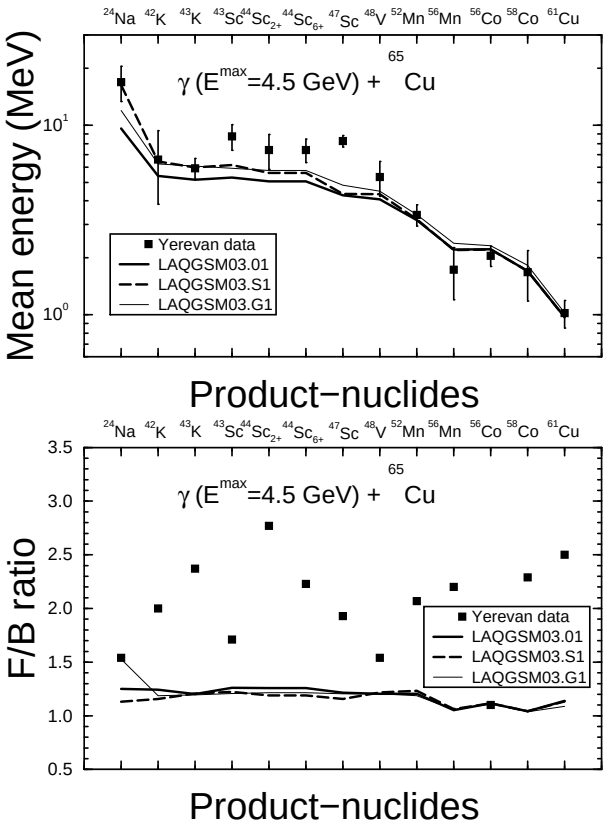

Figure 6. The measured data [32] for the mean laboratory kinetic energy and the R=F/B ratio of the forward product cross sections to the backward ones for the same reaction as shown in Fig. 5, but compared with results by LAQGSM03.01 and its "S" and "G" versions for only the measured products (listed on the top of both plots), isotope-by-isotope.

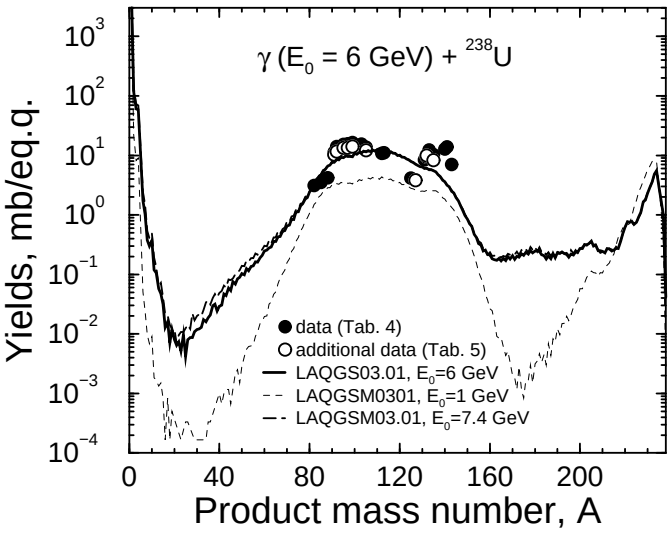

Figure 7. Comparison of measured (filled circles) [34, 35] mass distribution of the nuclides produced by E^{max} = 6 GeV bremsstrahlung photons on ^{238}U with results by LAQGSM03.01 (thick solid line). Open circles show some additional experimental data measured at other energies and compiled from the literature in Tab. 5 of Ref. [34]; results by LAQGSM03.01 at E^{max} = 1.0 to 7.4 GeV are shown for comparison by thin and thick dashed lines, respectively.

Acknowledgment

We are grateful to Dr. Igor Pshenichnov for sending us the γp and γn event generators from their Moscow photonuclear reaction INC [19] and thank our collaborators Drs. Arnie Sierk, Richard Prael, Nikolai Mokhov, and Mircea Baznat for useful discussions. This work was supported by the U. S. Department of Energy and by the Moldovan-U. S. Bilateral Grants Program, CRDF Project MP2-3045. SGM acknowledge partial support from a NASA Astrophysics Theory Program grant.

References

[1] S. G. Mashnik, M. I. Baznat, K. K. Gudima, A. J. Sierk, R. E. Prael, E-print: nucl-th/0503061; J. Nucl. Radiochem. Sci. **6** (2005) A1 (nucl-th/0503061).
[2] S. G. Mashnik, K. K. Gudima, A. J. Sierk, M. I. Baznat, N. V. Mokhov, LANL Report LA-UR-05-7321, Los Alamos (2005); RSICC Code Package PSR-532, http://www-rsicc.ornl.gov/codes/psr/psr5/psr-532.html.
[3] K. K. Gudima, S. G. Mashnik, A. J. Sierk, LANL Report LA-UR-01-6804, Los Alamos, 2001.
[4] S. G. Mashnik, K. K. Gudima, R. E. Prael, A. J. Sierk, Proc. 10th Int. Conf. on Nuclear Reaction Mechanisms, Varenna, Italy, 2003, p. 569 (nucl-th/0308043).
[5] S. G. Mashnik, K. K. Gudima, R. E. Prael, A. J. Sierk, Proc. of the Workshop on Nucl. Data for the Transmutation of Nuclear Waste, GSI, Germany, 2003, http://www-wnt.gsi.de/tramu/ (nucl-ex/0403056).
[6] S. G. Mashnik, K. K. Gudima, I. V. Moskalenko, R. E. Prael, A. J. Sierk, Adv. Space Res. **34** (2004) 1288 (nucl-th/0210065).
[7] S. G. Mashnik, A. J. Sierk, K. K. Gudima, M. I. Baznat, J. Phys.: Conf. Series **41** (2006) 340 (nucl-th/0510070).
[8] S. G. Mashnik, K. K. Gudima, M. I. Baznat, A. J. Sierk, R. E. Prael, N. V. Mokhov, LANL Report LA-UR-05-2686, Los Alamos, 2005.
[9] S. G. Mashnik, K. K. Gudima, M. I. Baznat, A. J. Sierk, R. E. Prael, N. V. Mokhov, LANL Report LA-UR-06-1764, Los Alamos, 2006; S. G. Mashnik, K. K. Gudima, and M. I. Baznat, LANL Report LA-UR-06-1955, Los Alamos, 2006 (nucl/th-0603046).
[10] S. Furihata, Nucl. Instr. Meth. **B171** (2000) 252; Ph.D. thesis, Tohoku University, Japan, 2003.
[11] R. J. Charity *et al.*, Nucl. Phys. **A483** (1988) 371 and references therein.
[12] J. P. Bondorf, A. S. Botvina, A. S. Iljinov, I. N. Mishustin, K. Sneppen, Phys. Rep. **257** (1995) 133.
[13] N. S. Amelin, K. K. Gudima, V. D. Toneev, Sov. J. Nucl. Phys. **52** (1990) 1722 and references therein.
[14] http://mcnp-green.lanl.gov/about_mcnp5.html.
[15] http://www-ap.fnal.gov/MARS/.
[16] http://mcnpx.lanl.gov/.
[17] K. K. Gudima, A. S. Iljinov, V. D. Toneev, Communication JINR P2-4661, Dubna, 1969.
[18] J. S. Levinger, Phys. Rev. **84** (1951) 43; Phys. Lett. **B82** (1979) 181.
[19] A. S. Iljinov, I. A. Pshenichnov *et al.*, Nucl. Phys. **A616** (1997) 575.
[20] P. Corvisiero *et al.* NIM **A346** (1994) 433.
[21] V. D. Toneev and K. K. Gudima, Nucl. Phys. A**400** (1983) 173c.
[22] N. Amelin, CERN/IT/ASD Report CERN/IT/99/6, Geneva, Switzerland: http://wwwinfo.cern.ch/asd/geant4/G4UsersDocuments/UsersGuides/PhysicsReferenceManual/html/ PhysicsReferenceManual.html.
[23] D. N. Olson, Ph.D. thesis, Cornell University, 1960.
[24] D. H. Boal and R. M. Woloshin, Phys. Rev. **C23** (1981) 1206.
[25] J. L. Matthews and W. Turchinetz, LNS Internal Report No. 110, 1966.
[26] K. V. Alanakyan *et al.*, Sov. J. Nucl. Phys. **25** (1977) 292.
[27] K. V. Alanakyan *et al.*, Sov. J. Nucl. Phys. **34** (1981) 828; Nucl. Phys. **A367** (1981) 429.
[28] K. Sh. Egiyan, Yerevan Physics Institute Preprint EFI-481(24)-81, Yerevan, 1981.
[29] K. V. Alanakyan *et al.*, Yerevan Physics Institute Preprint EFI-481(24)-81, Yerevan, 1981; JETP Lett. **32** (1980) 652; Sov. J. Nucl. Phys. **34** (1981) 50.
[30] S. G. Mashnik, Nucl. Phys. **A568** (1994) 703.
[31] G. A. Vartapetyan *et al.*, Sov. J. Nucl. Phys. **34** (1981) 163.
[32] A. A. Arakelyan *et al.*, Nucl. Phys. **A534** (1991) 535.
[33] A. R. Balabekyan *et al.*, E-print: nucl-ex/0603022, v2, 17 May 2006, submitted to Nucl. Phys. A.
[34] G. Andersson *et al.*, Nucl. Phys. **A197** (1972) 44.
[35] B. Schroder, Nucl. Phys. **A197** (1972) 88.